Development of a bunch-width monitor for low-intensity muon beam below a few MeV

Yuki Sue,[1,*] Mai Yotsuzuka,[1] Kenta Futatsukawa,[2] Kazuo Hasegawa,[3] Toru Iijima,[1,4] Hiromi Iinuma,[5] Kenji Inami,[1] Katsuhiro Ishida,[6] Naritoshi Kawamura,[2] Ryo Kitamura,[3] Yasuhiro Kondo,[3,5] Tsutomu Mibe,[2] Yasuhiro Miyake,[2] Takatoshi Morishita,[3] Yuga Nakazawa,[5] Masashi Otani,[2] Naohito Saito,[7] Koichiro Shimomura,[2] Yusuke Takeuchi,[8] Takahiro Ushizawa,[9] Takayuki Yamazaki,[2] and Hiromasa Yasuda[10]

[1]*Graduate School of Science, Nagoya University, Nagoya, Aichi 464-8602, Japan*
[2]*High Energy Accelerator Research Organization (KEK), Tsukuba, Ibaraki 305-0801, Japan*
[3]*Japan Atomic Energy Agency (JAEA), Tokai, Naka, Ibaraki 319-1195, Japan*
[4]*Kobayashi-Maskawa Institute (KMI), Nagoya University, Nagoya, Aichi 464-8602, Japan*
[5]*Graduate School of Science and Engineering, Ibaraki University, Mito, Ibaraki 310-8512, Japan*
[6]*Riken, Wako, Saitama 351-0198, Japan*
[7]*J-PARC Center, Tokai, Naka, Ibaraki 319-1195, Japan*
[8]*Graduate School of Science, Kyushu University, Fukuoka 819-0395, Japan*
[9]*SOKENDAI (The Graduate University for Advanced Studies), Hayama, Kanagawa 240-0193, Japan*
[10]*Graduate School of Science, University of Tokyo, Hongo, Tokyo 171-8501, Japan*

(Received 1 December 2019; accepted 21 January 2020; published 12 February 2020)

A destructive monitor to measure the longitudinal bunch width of a low-energy and low-intensity muon beam was developed. This bunch-width monitor (BWM) employed microchannel plates to detect a single muon with high time resolution. In addition, constant-fraction discriminators were adopted to suppress the time-walk effect. The time resolution was measured to be 65 ps in rms using a picosecond-pulsed laser. This resolution satisfied the requirements of the muon linac of the J-PARC E34 experiment. We measured the bunch width of negative-muonium ions ($\mu^+e^-e^-$) accelerated with a radio-frequency quadrupole using the BWM. The bunch width was successfully measured to be $\sigma = 0.54 \pm 0.11$ ns, which is consistent with the simulation.

DOI: 10.1103/PhysRevAccelBeams.23.022804

I. INTRODUCTION

The feasibility of muon accelerators is increasing considering the recent advances in high-intensity muon beams and efficient muon cooling. In the near future, H-line, a high-intensity muon beamline at the muon science facility (MUSE) [1] of Japan Proton Accelerator Research Complex (J-PARC), will provide a hundred million surface muons per second [2]. A muon beam cooling by the ionization of an absorber was recently demonstrated at the Muon Ionization Cooling Experiment in Rutherford Appleton Laboratory [3,4]. As another cooling method, the use of laser ionization to create atoms of muonium (μ^+e^-) enables the muons to be efficiently cooled to the kinetic energy of the thermal level of 25 meV [5,6]. By accelerating these cooled muons, a transmission muon microscope with a muon microbeam can be realized that will provide novel imaging in materials and life sciences [7]. In elementary particle physics, the J-PARC E34 experiment [8], which aims to precisely measure the anomalous magnetic moment $(g-2)_\mu$ and electric dipole moment of the muon, requires a high energy muon accelerator to obtain a low-emittance muon beam.

In the E34 experiment, muons are accelerated up to a kinetic energy of 212 MeV using four types of radio-frequency (rf) linear accelerators (linacs) depending on the beam velocity [9–12]. We previously demonstrated the first stage of muon acceleration using a prototype radio-frequency quadrupole linac (RFQ), which is the first rf structure with an operation frequency of 324 MHz [13].

As the next step, a beam test to accelerate muons by a few MeV is being planned. In this test, the actual RFQ for the muon linac and the prototype of the successive interdigital H-mode drift-tube linac (IH-DTL) [14] with an operating frequency of 324 MHz will be used. The longitudinal beam profile matching from the RFQ to the IH-DTL is particularly crucial owing to the small acceptance attributed to the alternating phase focusing scheme

*ysue@hepl.phys.nagoya-u.ac.jp

employed by the IH-DTL [10]. Therefore, the bunch length at the IH-DTL entrance must be measured precisely. Likewise, the bunch length at the exit of the IH-DTL needs to be measured for the verification of the acceleration as designed.

To this end, we developed a bunch-width monitor that can be used even with an extremely low-intensity beam. In the case of the muon linac, the intensity would be very low in the commissioning stage; for example, it was 5×10^{-4} μ^+/s in the acceleration demonstration using the prototype RFQ [13]. It is difficult to use collective methods such as fast current transformers or streak cameras [15–18] for such low-intensity and low-energy (less than a few MeV) beams. To overcome this, we developed a bunch-width monitor by measuring the time of flight (TOF) of a single muon for each event with high precision. This method limits the number of muons that can be detected in one macro pulse to one at most; that is, there is an intensity limit for this method. In the case of the proposed muon linac, ten muons per second are expected. Even with this rate, the measurement time is only several minutes; thus, the intensity limit of this method itself does not prevent effective beam tuning.

This bunch-width monitor (BWM) employed multi-anode microchannel plate (MCP) and constant-fraction discriminators (CFDs) [19]. An MCP has high sensitivity to low-energy single muons [20,21]. In addition, we focused on the high time response of an MCP. We measured the time resolution of the BWM using a pico-second-pulsed laser at a test bench and demonstrated the bunch width measurement with muons accelerated by the prototype RFQ.

This paper is organized into four sections. The next section shows the design of the BWM and the results of the evaluation of time resolution. Section III describes the principles used to measure the bunch width of muons accelerated with the RFQ using the BWM. The conclusions of this paper are presented in Sec. IV.

II. BUNCH-WIDTH MONITOR

The main principle of the proposed BWM is to perform single-event particle detection in low-intensity muon beams. Figure 1 shows a time structure of our muon linac. The reference signal is synchronized with a phase of the operation rf to determine the time origin. The width of a microbunch is measured by piling up the measured time modulo the rf period, 3.09 ns. Thus, not only the bunch width but also the bunch shape can be measured with this monitor in principle.

This method requires the ability to detect a single muon with the time resolution of a few percent of 324 MHz, which corresponds to less than 100 ps. A schematic diagram of the BWM is shown in Fig. 2. The BWM comprises MCP, CFD, reference signal input, and data acquisition modules.

The employed MCP assembly (Hamamatsu Photonics F1217-11G [22]) contained a two-stage MCP and four-strip anodes. The thickness of each MCP was 480 μm and the diameter of the round effective area was 42 mm. The diameter and bias angle of the microchannels were 12 μm and 12°, respectively. Negative high voltages were applied to both sides of the MCP (V_{in} and V_{out}) and the anodes were held at the ground potential. A charged particle entering a microchannel induces secondary-electron multiplication, and the typical gain through the two-stage MCP was found to be 10^6–10^7. The four-strip anodes were assigned as shown in Fig. 3. Because this monitor was located downstream of a bending magnet in the demonstration described in a later section, the strip anodes reduced the time uncertainty depending on the transverse spread caused by momentum dispersions. Multiple anodes reduced the hit occupancy and supplied coarse position information.

The signal-processing electronics of the CFD, which were adopted from the technology of the high-energy physics experiment [23], measured the timing of the MCP signal. The CFD picked off the timing at a constant fraction of the pulse height, which suppressed the charge-dependent time uncertainty, namely, time walk, which dominates the time uncertainty of the whole system. Time-to-digital converters (TDCs, CAEN V1290A [24]) with a least-significant bit of 24.4 ps and a time resolution of 35 ps were used to acquire the time information. The pulse height information was used to distinguish the muon

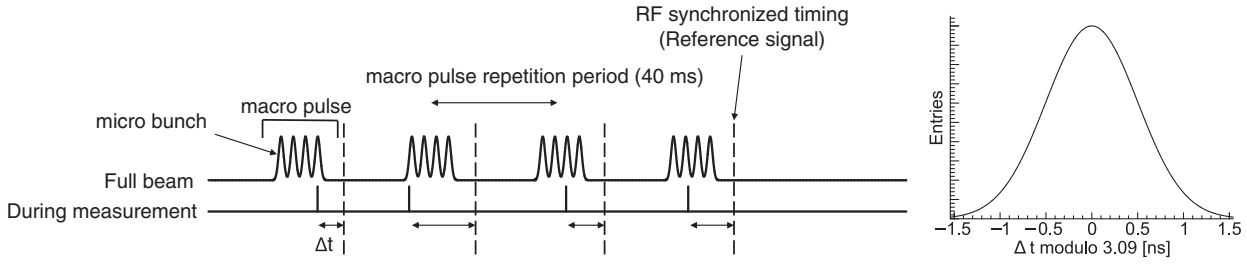

FIG. 1. Schematic of the muon beam structure. The intensity limits the measurement to the order of one muon per macro pulse to measure the bunch width using this method. The monitor measures the time difference between the one muon included in a pulse and reference timing, Δt. An example of the microbunch structure (left) and Δt distribution modulo rf period of 3.09 ns (right).

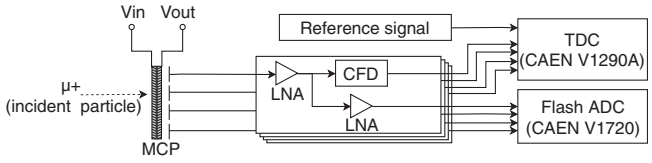

FIG. 2. Schematic diagram of the BWM. LNA stands for low-noise amplifier.

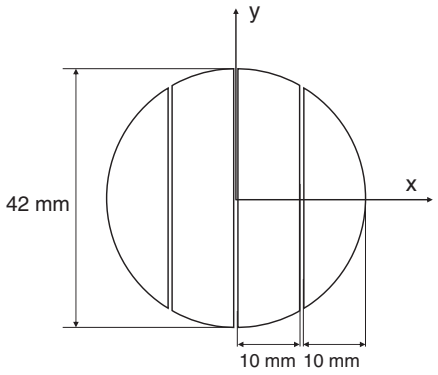

FIG. 3. Anode arrangement of the MCP. X- and y-axes correspond to the beam coordinate system.

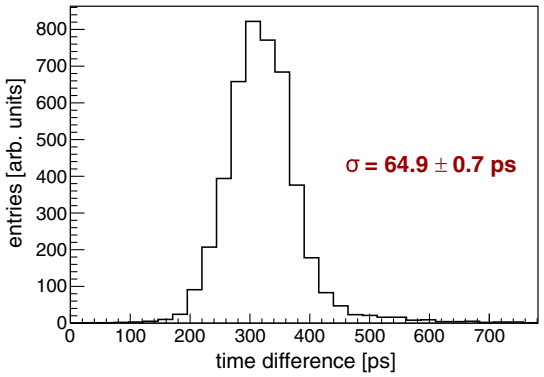

FIG. 4. Distribution of time difference on the TDC between the MCP signal and laser-synchronized signal. The standard deviation of the distribution corresponds to the time resolution of the BWM. This result was obtained with the typical HV setting, $V_{\mathrm{in}} = -2320$ V and $V_{\mathrm{out}} = -480$ V.

signal from the positron background. Other signal processing electronics using flash-analog-to-digital converters (FADCs, CAEN V1720 [24]) with a sampling rate of 250 MS/s were used to acquire the MCP waveforms.

The time resolution of the BWM was evaluated using the picosecond-pulsed laser in the offline test [25]. The time distribution of the MCP signal induced by the photoelectrons is shown in Fig. 4. The standard deviation of the distribution was found to be 65 ps. The values on each of the four anodes were comparable. Because it included the laser pulse width, $\sigma = 34$ ps at minimum, the time resolution of the BWM itself was estimated to be less than 65 ps, which corresponds to a phase resolution of 2% [25]. The time resolution was not significantly different within the range of $V_{\mathrm{in}} = -2320$ to -2100 V. The estimated resolution satisfied the requirement for the J-PARC E34 experiment.

III. DEMONSTRATION OF BUNCH-WIDTH MEASUREMENT

To demonstrate the bunch-width measurement using the BWM, we measured a negative muonium ion (Mu^-, $\mu^+e^-e^-$) accelerated by the RFQ. The experiment was conducted at the multipurpose muon experimental area (MUSE D2 area) in the Materials and Life Science Facility (MLF) of J-PARC.

A. Experimental setup

The experimental setup, which was modified from the Mu^- acceleration setup [13], is shown in Fig. 5. The rapid cycling synchrotron (RCS) provided proton bunches to a muon production target of the MLF with a repetition rate of 25 Hz. The μ^+ beam intensities were 2.5×10^6 and 4.0×10^6/s when the proton beam powers were 300 and 500 kW, respectively. The size of the Mu^- production target was 86×82 mm^2. The muons were injected into the RFQ using an electrostatic lens system called a Soa lens [26]. They were then accelerated with the RFQ. The beam accelerated to 89 keV was transferred through two quadrupole magnets (QM1 and QM2) with respective field gradients of 2.0 and 1.8 T/m and a quarter-wave resonator buncher cavity [27] with a maximum energy gain of 5.3 keV. QM1 was focused in the X-direction and QM2 was focused in the Y-direction. The buncher cavity had two gaps, where the synchronized particle passed at $-90°$ relative to the crest; thus, it experienced no acceleration or deceleration field. The 89 keV Mu^-'s were deflected horizontally by 45° through a bending magnet (BM) and were detected using the MCP of the BWM.

The parameters of the beamline were determined on the basis of simulations. The beam transport parameters in the Soa lens were calculated via GEANT4 simulation [28] and the RFQ was calculated with PARMTEQM [29]. The beam transfer from the exit of the RFQ to BWM was based on the PARMILA [30] and TRACE3D [31] simulation packages. The beam envelope calculated with TRACE3D [31] is shown in Fig. 6. The bunch width at the MCP of the BWM was estimated to be 0.47 ns in a standard deviation, whose full width was within the one rf period.

The diagram of the 324 MHz rf system is shown in Fig. 7. The rf pulse was generated by a signal generator (Tektronix TSG4104A [32]) and the generated signal was amplified by 324 Hz 5 kW-solid-state amplifier units (R&K CA324BW0.4-6767RP [33]). The rf power was transmitted via 50 Ω coaxial cables to the loop-type couplers of the RFQ and the buncher cavity. The rf powers applied to the

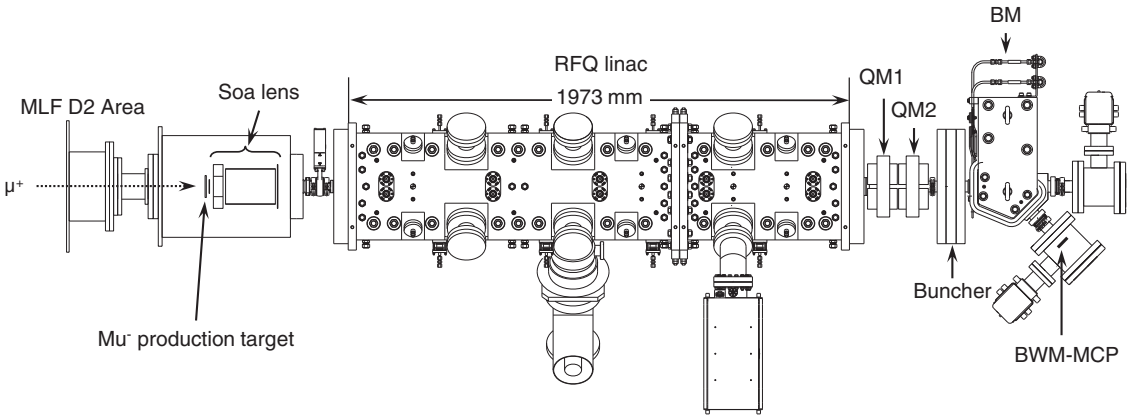

FIG. 5. Drawing of the apparatus to produce Mu^- bunches installed in the MLF MUSE D2 area at the J-PARC.

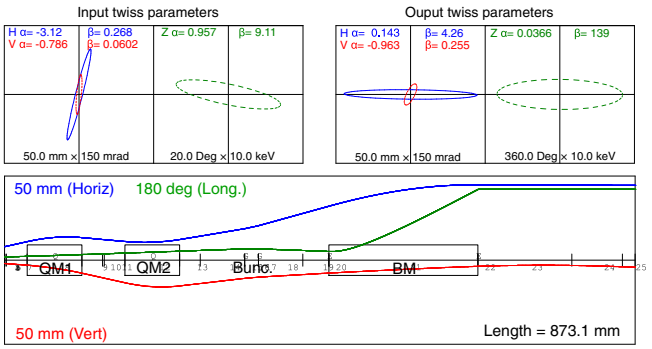

FIG. 6. Rms envelope calculation with TRACE3D [31] for the period from the RFQ exit to the MCP of the BWM. The units are in mm-mrad in the $x - x'$ and $y - y'$ phase planes and deg-keV in the $\Delta\phi - \Delta W$ phase plane.

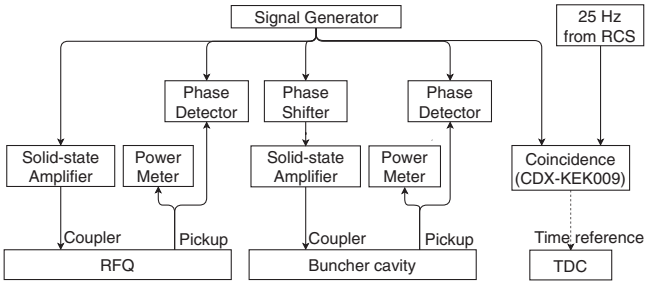

FIG. 7. Diagram of the 324 MHz rf system. Note that the broken-line arrows are not 324 MHz rf.

RFQ and buncher were 2.3 and 0.36 kW, respectively. A phase difference between the RFQ and buncher was controlled using a line-stretcher phase shifter according to the measured phases via pickup monitors using rf phase detectors (Nihon Koshuha [34]). These rf phase monitors were calibrated using a vector voltmeter with an accuracy of less than $\pm 0.8°$ in peak-to-peak over the entire phase difference range. The time-dependent instability of the phase difference was less than $\pm 3°$; thus, its effect on the bunch shape was sufficiently small.

The BWM data were acquired within a time window of 10 μs, which was triggered at 25 Hz. The high voltages applied to both sides of the MCP of the BWM were $V_{\text{in}} = -2160$ V and $V_{\text{out}} = -440$ V such that the dark current rate would not be too high. The reference signal of the BWM was synchronized with a phase of the rf applied to the RFQ. The 25 Hz trigger was synchronized with the phase of the rf signal using a CANDOX CDX-KEK009 module [35].

B. Data processing for signal extraction

The bunch width was measured using the TDC data after removing the main background events using the FADC data. The TOF and pulse height information extracted from the waveform of the MCP signal obtained with the FADC were used to reduce the background.

The main background comprised high-energy positrons from muon decay. The pulse height of the Mu^- signal on the MCP was higher than that of the decay positron event [13]. To extract the signal events, TOF was defined as the time difference from the muon arrival at the Mu^- production

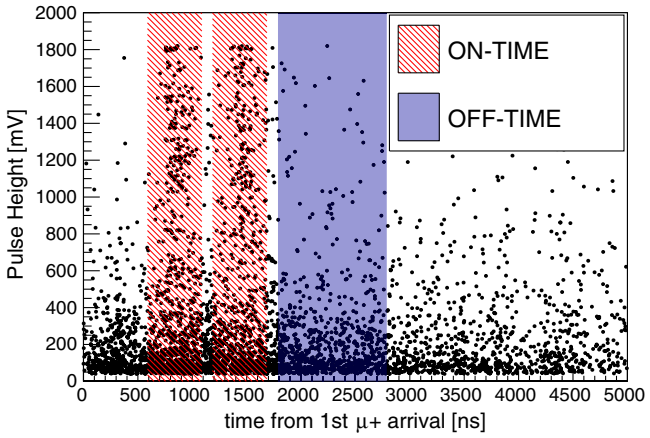

FIG. 8. TOF and pulse height distribution of the MCP signals of the BWM recorded using the FADC.

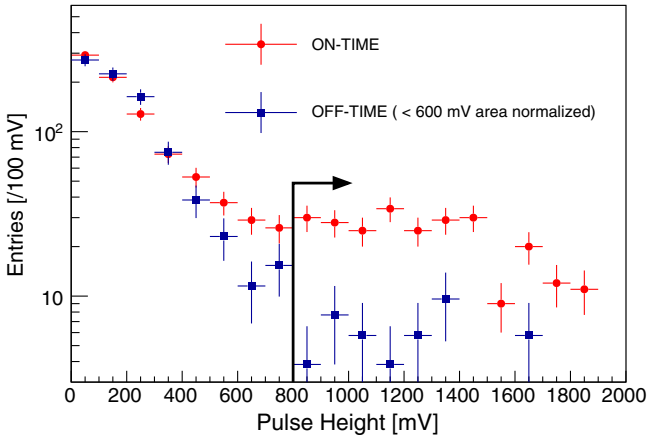

FIG. 9. Pulse height distribution of the signal-contained events (ON-TIME) and background events (OFF-TIME). The OFF-TIME events are normalized so that the number of OFF-TIME events whose pulse height is less than 600 mV is equal to that of the ON-TIME events. The applied pulse-hight cut of 800 mV is indicated with the solid line with the arrow.

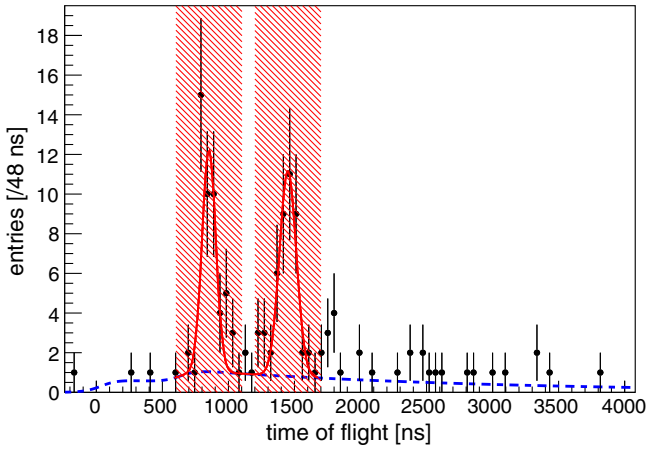

FIG. 10. TOF distribution after the application of pulse-height cut. The events in the hatched (red) bands were used for bunch width measurement.

target to Mu^- arrival at the MCP of the BWM. The TOF of the accelerated Mu^- was estimated to be 839 ns from the calculation based on the simulation. Figure 8 shows a scatter plot of the TOF and pulse height. The TOF periods where the accelerated Mu^- would be detected (ON-TIME) are drawn as two hatched (red) bands: the RCS was operated using two bunches at an interval of 598 ns. Figure 9 shows the comparison between the ON-TIME and background events (OFF-TIME) corresponding to the TOF period drawn as the solid (blue) band in Fig. 8. The enhancement appeared around the higher pulse height region in the ON-TIME events in comparison to the OFF-TIME events. Accordingly, the events with pulse heights higher than 800 mV were used. Figure 10 shows the TOF distribution after the pulse height

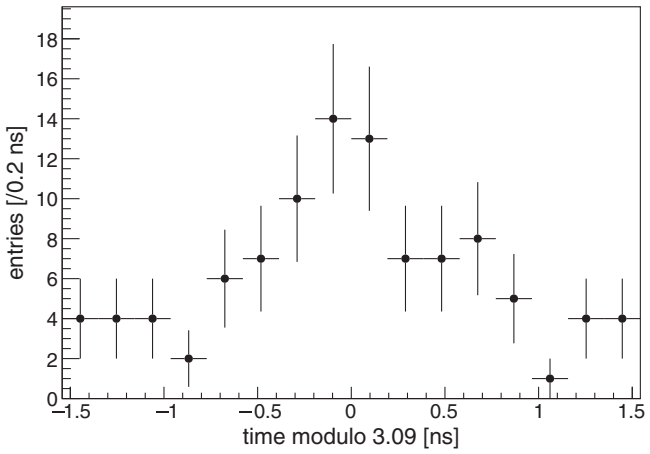

FIG. 11. Time difference distribution modulo 3.09 ns obtained using the TDC data.

cut, which enhances the TOF signal in accordance with the estimated TOF of Mu^- accelerated up to 89 keV.

C. Results

The TOF distribution was fitted with Gaussians. The signal regions were defined as TOF of ± 250 ns around the Gaussian peaks, shown as the hatched bands in Fig. 10. This band width corresponded to four sigma of the fitted Gaussians. Figure 11 shows the time difference distribution modulo the rf period of 3.09 ns after using the pulse-height and TOF cuts. The number of residual background events in this plot were estimated from a fitting to the background region of the TOF distribution, which is composed of the side bands of the TOF signal region. The likelihood-fit result of the background is drawn as a broken line in Fig. 10.

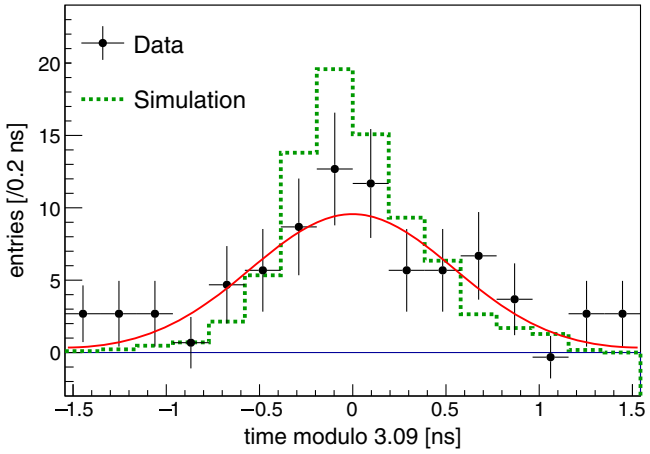

FIG. 12. Bunch width measurement results. The black data points with error bars indicate the data including background subtraction based on the pulse-height cuts. The broken line indicates the simulated value. The solid line is a result of Gaussian fitting. The event number in the simulation was normalized to the experimental data. The range of the horizontal axis corresponds to a period of the operating rf.

TABLE I. Comparison of the demonstration results and expected values. The expected bunch width is calculated from the simulation. The expected Mu^- rate and error are estimated by scaling the former experiment [13] with the beam power and transport efficiency.

	Expected	Measured
Bunch width [ns]	0.47	0.54 ± 0.11
Mu^- rate[/s]	$(6 \pm 1) \times 10^{-4}$	$(5.4 \pm 0.5) \times 10^{-4}$

The time constant of muon decay is 2.2 μs, which is sufficiently longer than the rf period; therefore, the time difference of this component modulo the rf period should be flat. Thus, the estimated background was subtracted from each bin of Fig. 11 and its error was added as a quadrature sum.

The bunch width measurement results after subtracting the estimated backgrounds are shown in Fig. 12. The 79 Mu^-'s were detected over a period of 40 h. The intensity of the detected Mu^- on the criteria was $(5.4 \pm 0.5) \times 10^{-4}$ Hz, which is consistent with the former experiment [13]. The bunch width was $\sigma = 0.54 \pm 0.11$ ns as a result of Gaussian fitting. The statistical uncertainty was dominant in this error, which was caused by the low efficiency of Mu^- production. This width was found to be consistent with the simulation value based on PARMILA. These results are summarized in Table I. This proves the fundamental utility of the method with the BWM to low-intensity and low-energy muon beams.

IV. CONCLUSION

A BWM to measure the bunch width of low-intensity and low-energy muon beams with high time resolution was developed for the 324 MHz muon linac. The time resolution of the BWM was $\sigma = 65$ ps. The measurement of the bunch width of the Mu^- accelerated up to 89 keV with the RFQ linac was demonstrated. The value of σ was found to be 0.54 ± 0.11 ns, which is consistent with the result of simulated bunch width. These results indicate that the BWM can measure the bunch width of low-intensity, 10^{-4} μ/ s, and low-energy, 89 keV, muon beams with a phase resolution of less than 2%; this satisfies the requirement for the measurement at a matching section of the RFQ and IH-DTL in the muon linac. The developed BWM allows us to perform beam commissioning to accelerate muons up to a few MeV with a successive IH-DTL linac.

ACKNOWLEDGMENTS

We express our appreciation to TIME Co., Ltd., who fabricated the buncher cavity. This work was supported by JSPS KAKENHI Grants No. JP15H03666, JP15H05742, JP16H03987, JP16J07784, JP18H03707, JP18H05226, and JP19J21763. This experiment at the Materials and Life Science Experimental Facility of the J-PARC was performed under user programs (Proposal No. 2018A0222).

[1] Y. Miyake *et al.*, J-PARC muon facility, MUSE, J. Phys. Conf. Ser. **225**, 012036 (2010).
[2] N. Kawamura *et al.*, New concept for a large-acceptance general-purpose muon beamline, Prog. Theor. Exp. Phys. **2018**, 113G01 (2018).
[3] D. Adams *et al.* (MICE Collaboration), First particle-by-particle measurement of emittance in the Muon Ionization Cooling Experiment, Eur. Phys. J. C **79**, 257 (2019).
[4] M. Bogomilov *et al.* (MICE Collaboration), First demonstration of ionization cooling by the Muon Ionization Cooling Experiment, Nature (London) **578**, 53 (2020).
[5] K. Nagamine, Y. Miyake, K. Shimomura, P. Birrer, J. P. Marangos, M. Iwasaki, P. Strasser, and T. Kuga, Ultraslow Positive-Muon Generation by Laser Ionization of Thermal Muonium from Hot Tungsten at Primary Proton Beam, Phys. Rev. Lett. **74**, 4811 (1995).
[6] G. A. Beer *et al.*, Enhancement of muonium emission rate from silica aerogel with a laser-ablated surface , Prog. Theor. Exp. Phys. **2014**, 091C01 (2014).
[7] Y. Miyake, Y. Nagatani, T. Yamazaki, and P. Strasser, 2pM_PL2 Transmission Muon Microscope by muon microbeam, realizing 3-D Imaging, Microscopy **67**, i3 (2018).
[8] M. Abe *et al.*, A new approach for measuring the muon anomalous magnetic moment and electric dipole moment, Prog. Theor. Exp. Phys. **2019**, 053C02 (2019).
[9] Y. Kondo *et al.*, Simulation study of muon acceleration using RFQ for a new muon g-2 experiment at J-PARC, in *Proceedings of IPAC2015, Richmond, VA, USA* (JACoW, Geneva, Switzerland, 2015), p. 3801, https://doi.org/10.18429/JACoW-IPAC2015-THPF045.
[10] M. Otani, T. Mibe, M. Yoshida, K. Hasegawa, Y. Kondo, N. Hayashizaki, Y. Iwashita, Y. Iwata, R. Kitamura, and N. Saito, Interdigital H-mode drift-tube linac design with alternative phase focusing for muon linac, Phys. Rev. Accel. Beams **19**, 040101 (2016).
[11] M. Otani *et al.*, Disk and washer coupled cavity linac design and cold-model for muon linac, J. Phys. Conf. Ser. **1350**, 012097 (2019).
[12] Y. Kondo, K. Hasegawa, M. Otani, T. Mibe, M. Yoshida, and R. Kitamura, Beam dynamics design of the muon linac high-beta section, J. Phys. Conf. Ser. **874**, 012054 (2017).
[13] S. Bae *et al.*, First muon acceleration using a radio-frequency accelerator, Phys. Rev. Accel. Beams **21**, 050101 (2018).
[14] Y. Nakazawa *et al.*, Development of inter-digital H-mode drift-tube linac prototype with alternative phase focusing for a muon linac in the J-PARC muon G-2/EDM experiment, J. Phys. Conf. Ser. **1350**, 012054 (2019).
[15] G. Shen and M. Ikegami, Tuning of RF amplitude and phase for the separate-type drift tube linac in J-PARC, Nucl. Instrum. Methods Phys. Res., Sect. A **598**, 361 (2009).
[16] A. V. Feschenko, in *Proceedings of the 19th Particle Accelerator Conference, Chicago, IL, 2001* (IEEE, Piscataway, NJ, 2001), p. 517.
[17] A. Miura, J. Tamura, Y. Liu, and T. Miyao, Bunch shape monitor development in J-PARC linac, J. Phys. Conf. Ser. **874**, 012080 (2017).
[18] A. T. Margaryan, RF timing technique and its possible applications, Armenian J. Phys. **2**, 164 (2009).

[19] B. Leskovar and C. C. Lo, Single photoelectron time spread measurement of fast photomultipliers, Nucl. Instrum. Methods Phys. Res., Sect. A **123**, 145 (1975).
[20] B. Kim *et al.*, Development of a microchannel plate based beam profile monitor for a re-accelerated muon beam, Nucl. Instrum. Methods Phys. Res., Sect. A **899**, 22 (2018).
[21] M. Otani *et al.*, Response of microchannel plates to positrons from muon-decays, Nucl. Instrum. Methods Phys. Res., Sect. A **943**, 162475 (2019).
[22] HAMAMATSHU PHOTONICS K. K., https://www.hamamatsu.com.
[23] K. Inami (Belle-II PID Group), TOP counter for particle identification at the Belle II experiment, Nucl. Instrum. Methods Phys. Res., Sect. A **766**, 5 (2014).
[24] CAEN S. p. A., https://www.caen.it.
[25] M. Yotsuzuka *et al.*, Development of the longitudinal beam monitor with high time resolution for a Muon LINAC in the J-PARC E34 experiment, in *Proceedings of IPAC2019, Melbourne, Victoria Australia* (JACoW Publishing, Geneva, Switzerland, 2019), p. 2571, https://doi.org/10.18429/JACoW-IPAC2019-WEPGW042.
[26] S. Berko *et al.*, *Positron Studies of Solids, Surfaces, and Atoms: A Symposium to Celebrate Stephan Berko's 60th Birthday, Brandeis University, December 12, 1984* (World Scientific, Singapore, 1986), p. 199.
[27] M. Otani *et al.*, Compact buncher cavity for muons accelerated by a radio-frequency quadrupole, Nucl. Instrum. Methods Phys. Res., Sect. A **946**, 162693 (2019).
[28] S. Agostinelli *et al.* (GEANT4 Collaboration), Geant4–a simulation toolkit, Nucl. Instrum. Methods Phys. Res., Sect. A **506**, 250 (2003).
[29] K. R. Crandall, R. H. Stokes, and T. P. Wangler, Los Alamos Report No. LA-UR-96-1836, 1996.
[30] H. Takeda, Los Alamos Report No. LA-UR-98-4478, 1998.
[31] K. R. Crandall and D. P. Rusthoi, Los Alamos Report No. LA-UR-97-886, 1997.
[32] Tektronix Inc., http://www.tek.com/.
[33] R & K Co. Ltd., http://www.rk-microwave.com.
[34] Nihon Koshuha Co. Ltd., http://www.nikoha.co.jp.
[35] CANDOX Systems Inc., http://www.candox.co.jp.